Neurobiology of Disease 92 (2016) 46–54

Contents lists available at ScienceDirect

Neurobiology of Disease

journal homepage: www.elsevier.com/locate/ynbdi

Review

Reprint of "Hypomyelinating disorders: An MRI approach☆

A. James Barkovich [a,*], Sean Deon [b]

[a] Neuroradiology Section, Department of Radiology and Biomedical Imaging, UCSF-Benioff Children's Hospital, San Francisco, Q6 CA, United States
[b] University of Colorado Medical Center and Prof. Petra Pouwels, University of Amsterdam

ARTICLE INFO

Article history:
Received 12 August 2015
Revised 10 October 2015
Accepted 14 October 2015
Available online 24 May 2016

Keywords:
Hypomyelinating disorders
Genetic leukoencephalopathies
Dysmyelinating and demyelinating disorders

ABSTRACT

In recent years, the concept of hypomyelinating disorders has been proposed as a group of disorders with varying systemic manifestations that are identified by MR findings of absence or near absence of the T2 hypointensity that develops in white matter as a result of myelination. Initially proposed as a separate group because they were the largest single category of undiagnosed leukodystrophies, their separation as a distinct group that can be recognized by looking for a specific MRI feature has resulted in a marked increase in their diagnosis and a better understanding of the different causes of hypomyelination. This review will discuss the clinical presentations, imaging findings on standard MRI, and new MRI-related techniques that allow a better understanding of these disorders and proposed methods for quantifying the myelination as a potential means of assessing disease course and the effects of proposed treatments.

Disorders with hypomyelination of white matter, or hypomyelinating disorders (HMDs), represent the single largest category among undiagnosed genetic leukoencephalopathies (Schiffmann and van der Knaap, 2009; Steenweg et al., 2010). This group of inborn errors of metabolism is characterized by a magnetic resonance imaging (MRI) appearance of reduced or absent myelin development: delay in the development of T2 hypointensity and, often, T1 hyperintensity in the white matter of the brain. The concept of hypomyelination was first conceptualized by (Schiffmann and van der Knaap, 2009; Steenweg et al., 2010; Schiffmann et al., 1994) in a series of papers that showed that these MRI characteristics were easily recognized, were different from the MRI characteristics of dysmyelinating and demyelinating disorders, and that the combination of these imaging findings with specific other clinical and imaging features could be used to make diagnoses with some confidence. In this manuscript, we will discuss the physiologic and genetic bases of hypomyelinating disorders, as well as their classification, clinical manifestations and imaging characteristics.

Contents

1. Hypomyelination disorders: clinical and MRI Phenotypes

The prototype hypomyelinating disorder, *Pelizaeus–Merzbacher disease* (PMD), is caused by mutations of the *PLP1* gene, which encodes proteolipid protein, one of the principal structural proteins of myelin (Koeppen et al., 1987; LeVine et al., 1990; Sistermans et al., 1998). Pathogenesis is believed to be oligodendrocyte death via an unfolded protein response to *PLP1* mutations (Southwood et al., 2002; Dhaunchak et al., 2011), possibly due to depletion of molecular chaperones from the

☆ A publisher's error resulted in this article appearing in the wrong issue. The article is reprinted here for the reader's convenience and for the continuity of the special issue. For citation purposes, please use the original publication details Neurobiology of Disease 87 (2016) 50–58.
DOI of original article: http://dx.doi.org/10.1016/j.nbd.2015.10.015.

* Corresponding author.
E-mail address: james.barkovich@ucsf.edu (A.J. Barkovich).

Available online on ScienceDirect (www.sciencedirect.com).

http://dx.doi.org/10.1016/j.nbd.2015.10.022
0969-9961/

endoplasmic reticulum and fragmentation of the Golgi apparatus (Numata et al., 2013). Affected patients (almost exclusively boys) show early delays in motor development, almost always associated with nystagmus during the first year, choreoathetosis or ataxia of the head and trunk in the second half of the first year, and progressive spasticity (frequently associated with dystonia) that begins in early childhood. Development typically plateaus during the second half of the first decade, followed by slow deterioration beginning in adolescence. More severely affected patients are considered to have the "connatal form" of the disease, achieving almost no motor milestones. Hypotonia, feeding problems and absent primitive reflexes are common in the neonatal period. Nystagmoid ocular movements and extrapyramidal hyperkinesia are followed by the development of epilepsy, and early ataxia is followed by severe dystonia, impaired growth, and early death, usually by the end of the first decade (van der Knaap and Valk, 2005a; Boespflug-tanguy, 2013). A smaller percentage of patients with *PLP1* mutations (~10%) will develop a phenotype of *spastic paraplegia type 2* (SPG2) (van der Knaap and Valk, 2005a; Boespflug-tanguy, 2013; Garbern et al., 1999), exhibiting delayed early motor development, with progressive gait abnormalities over the first 5 postnatal years followed by development of ataxia, spasticity and loss of ambulation by the middle teen years. A slightly more severe variant of SPG2 has been recently described, caused by mutations of *PLP1* either in the PLP1-specific region encoded by exon 3B (this region is normally spliced out in the formation of DM20) or in PLP1 intron 3. These mutations cause hypomyelination of the early myelinated axons in the medulla, the lower pons (at the border of the medulla) and the hilus of the cerebellar dentate nuclei (Kevelam et al., 2015). Affected patients presented during the first or second year of life with nystagmus, or in early childhood with cerebellar dysfunction or developmental delay, followed during childhood by development of progressive spasticity or cerebellar dysfunction (Kevelam et al., 2015). See Table 1 for features of diseases.

Pelizaeus–Merzbacher-like disease (PMLD), also called hypomyelinating leukodystrophy type 2 and *GJC2*-related disorders, is caused by mutations of the gap junction protein, gamma-2 (*GJC2*) gene at chromosome 1q42.13, which is expressed specifically in oligodendrocytes in parallel with other myelin genes (Menichella et al., 2003). Affected patients present with clinical features similar to those found in less severe forms of PMD, accompanied by a mild peripheral neuropathy (Uhlenberg et al., 2004). Most reported patients present with nystagmus, impaired motor development, ataxia, dysarthria and a movement disorder, but have learned to walk, to talk and have normal cognition (Biancheri et al., 2013; Meyer et al., 2011). Some, however, never develop language and never walk independently (Gotoh et al., 2014); it is likely that outcomes depend upon the type and location of the mutation and its effect upon the function of the protein product in specific molecular pathways. Imaging findings are essentially identical to those of PMD (Steenweg et al., 2010; Gotoh et al., 2014).

POL III related leukodystrophies (POL3) result from mutations of the polymerase III, RNA, subunit A (*POLR3A* at chromosome 10q22.3) and subunit B (*POLR3B* at chromosome 12q23.3) genes, which are suggested to regulate function of RNA polymerase III and its targets; dysfunction is thereby suggested to result in decreased expression of certain tRNAs during development, with impaired synthesis of myelin (and other) proteins (Gv et al., 2011). POL3 are characterized clinically by varying combinations of cerebellar ataxia, upper motor neuron signs, dental abnormalities and hypogonadotropic hypogonadism; intellectual disabilities are also common (Bernard and Vanderver, 2012; Daoud et al., 2013). Although it is suggested that affected patients may be classified as one of five (overlapping) clinical phenotypes (Bernard and Vanderver, 2012), and some patients with POLR3A mutations are reported to have 4 H syndrome (Bernard and Vanderver, 2012), a review of the literature suggests that POL3 are characterized clinically by three major clinical findings (motor dysfunction, dental abnormalities and hypogonadotropic hypogonadism) that are present in varying combinations together with MRI findings of hypomyelination, along with cerebellar atrophy and T2 hypointensity of the thalami and/or pallidum(Gv et al., 2011; Bernard and Vanderver, 2012; Daoud et al., 2013; La Piana et al., 2014; Wolf et al., 2005, 2007).

Table 1
Characteristics of hypomyelinating disorders.

Disorder/ abbreviation	OMIM	Gene	Heritance	Clinical	MRI
Pelizaeus–Merzbacher Dz/hereditary spastic paraparesis type 2	312920	*PLP1*	X-linked	Nystagmus, choreoathetosis, dystonia, spasticity. More severe in connatal form.	Homogeneous HM on T1, T2. Decreased FA, RD. Late atrophy.
Pelizaeus–Merzbacher like Dz	608804	*GJC2*	AR	Similar to PMD	Homogeneous HM including brainstem.
Pol III related leukodystrophies	607694, 614381	*POLR3A*, *POLR3B*	AR	Cerebellar signs, UMN signs, dental anomalies, HH.	Homogeneous HM. T2 HI of GP and Thalami, Cb atrophy
Oculodentodigital dysplasia	164200	*GJA1*	AD, sporadic	Characteristic facies, anomalies of dentition, eyes, digits of hands/ft, dysarthria, spasticity, ataxia, seizures	Homogeneous HM. Cb atrophy. T2 HI GP
Hypomyelination with congenital cataracts	610532	*FAM126A*	AR	Cataracts, congenital or childhood, variable delay in motor development.	Heterogeneous HM with higher T1 HI T2 HyI in periventricular WM, progressive atrophy
18q-syndrome	601808	*18q-*	Sporadic	Characteristic facies, sensorineural hearing loss, hypotonia, seizures, nystagmus, choreoathetosis	Regions of heterogeneous T2 HM. Cb hypoplasia.
Hypomyelination with atrophy of basal ganglia and cerebellum	612438	*TUBB4A*	Sporadic	DD, hypotonia, nystagmus, and extrapyramidal movement disorders	Homogeneous HM. Atrophy of putamen > Cb, caudate, cerebral WM.
TUBB4A-associated Hypomyelination	602662	*TUBB4A*	Sporadic	DD, hypotonia, nystagmus, slowly progressive spastic paraparesis	Isolated HM
Trichothiodystrophy with photosensitivity	601675	*ERCC2*, *ERCC3*, *GTF2H5*, *MPLKIP*	AR	DD, coarse and brittle hair, icthyosis, short stature, craniofacial dysmorphisms	Homogenous HM on T1, T2. Cb atrophy.
RARS-associated hypomyelination	609136	*RARS*	AR, AD	Motor delay, nystagmus, ataxia, dystonia	Homogeneous HM on T1, T2. Cerebral and Cb atrophy.
Hypomyelination with brain stem and spinal cord involvement	615281	*DARS*	AR	Motor delay, progressive spasticity of legs, nystagmus, +/− mild cognitive impairment	HM on T2 in cerebral WM, pons, ICP, CST, DSC

Abbreviations: HM = hypomyelination, DD = developmental delay, HH = hypogonadotropic hypogonadism, UMN = upper motor neuron, HI = Hypointensity, HyI = Hyperintensity, Ca++ = calcifications, CC = corpus callosum, IC = internal capsule, BS = brain stem, Cb = cerebellum, GP-globus pallidus, Thal = thalamus, CST = corticospinal tracts, ICP = inferior Cb peduncle, DSC = dorsal spinal columns, HSmegaly = hepatosplenomegaly, FA = fractional anisotropy, RD = radial diffusivity,

Oculodentodigital dysplasia (ODD) is an autosomal dominant disorder (sometimes sporadic), caused by mutations of the gap junction protein, alpha-1 (*GJA1*) gene at chromosome 6q22.31, which encodes connexin-43, an abundant transmembrane protein that is an important building blocks of gap junction channels (which connect the cytoplasm of neighboring cells) and non-junctional hemichannels in the plasma membranes of glia (which allow passage of transmitters that complement gap channel communication) (De Bock et al., 2013). Patients with ODD have a characteristic facial appearance with a narrow nose, thin nostrils, small anteverted nares and hypoplastic nasal alae in >90%, while hands (and sometimes feet) are characterized by syndactyly of the 4th and 5th digits in 80%; microphthalmia or microcornea is present in ~70% (Paznekas et al., 2009). When teeth erupt, they are characterized by microdontia and hypoplasia of enamel, while neurologic exam often reveals spasticity/hyperreflexia, dysarthria, ataxia and, sometimes, seizures (usually controlled with medications) (Paznekas et al., 2009). There appears to be no obvious correlation between *GJA1* genotype and specific ODDD phenotypic features. MRI findings show hypomyelination with T2 hypointensity of the globus pallidus and putamen, as well as cerebellar hypoplasia (Pouwels et al., 2014; Norton et al., 1995; Gutmann et al., 1991)..

Hypomyelination with congenital cataracts is a rare autosomal recessive disorder caused by mutations of the family with sequence similarity 126, member A (*FAM126A*) gene at chromosome 7p15.3, which encodes hyccin, a protein that appears to be essential for proper myelination of central and peripheral axons (Zara et al., 2006). Affected patients are characterized by congenital cataracts, progressive neurological impairment, and a deficiency of myelin in the central and peripheral nervous systems (Zara et al., 2006; Biancheri et al., 2007). Original descriptions considered the bilateral cataracts to be the most important finding, being present at birth while the neurodevelopmental disabilities evolved over the first two years (Zara et al., 2006). However, more recent studies have revealed that the cataracts may not be present at birth (or become detectable until the second or third year of life or later (Ugur and Tolun, 2008)) and that the motor findings are extremely variable in time of onset, despite the presence of similar mutations (Biancheri et al., 2011). In addition, more recent studies have shown a specific MRI pattern of hypomyelination with the T2 signal more increased in the periventricular white matter (as compared with subcortical and deep white matter), suggesting that MRI may be important in establishing the early diagnosis (Biancheri et al., 2011; Traverso et al., 2013).

The *18q deletion syndrome* (18q-syndrome) is an autosomal deletion disorder with variable phenotype depending upon the precise segment of the distal portion of chromosome 18q that is deleted. Most frequently, patients have short stature and abnormalities of the brain and head include mental retardation, microcephaly, midfacial hypoplasia, hypotelorism, epicanthus, high or cleft palate, and narrow or atretic ear canals with conductive or sensorineural hearing loss (van der Knaap and Valk, 2005b). Cognitive abilities vary from borderline to severely deficient, while neurological abnormalities include hypotonia, delayed motor milestones, seizures, nystagmus, tremor and choreoathetosis (van der Knaap and Valk, 2005b; Linnankivi et al., 2006). MRI shows a variable degree of hypomyelination; most commonly, T1 weighted images are nearly normal, with decreased hyperintensity in the subcortical white matter only, whereas T2 weighted images show the white matter to be diffusely hyperintense compared to the gray matter of the cerebral cortex and basal ganglia (van der Knaap and Valk, 2005b; Linnankivi et al., 2006). According to Linnankivi et al., the white matter T2 hyperintensity was present in individuals with terminal deletions, while most of those with interstitial deletions had normal MRIs (Linnankivi et al., 2006). It is not established whether the T2 changes represent hypomyelination or astrogliosis associated with accelerated myelin turnover (Tanaka et al., 2012; Tada and Takanashi, 2014); however, for the purposes of imaging analyses, 18q- syndrome should be in the differential diagnosis for MRI appearance of hypomyelination.

Hypomyelination with atrophy of the basal ganglia and cerebellum (HABC) was recently discovered to be associated with heterozygous mutations of the tubulin beta 4A (*TUBB4A*) gene at chromosome 19p13. Heterodimers of α-tubulin and β−tubulin undergo polymerization to form microtubules (Simons et al., 2013; Hamilton et al., 2014), which are critical structures for normal mitosis, neuronal morphogenesis, cell migration and for intracellular transport of proteins and neurotransmitters (Franker and Hoogenraad, 2013; Etienne-Manneville, 2013; Walczak et al., 2013; Sakakibara et al., 2013). Mutations in HABC patients seem to affect β−tubulin at its binding site with α-tubulin, suggesting that abnormal heterodimer formation/maintenance or abnormal heterodimer polymerization may be a root cause of the disorder. Clinically, HABC is characterized by onset in infancy to early childhood, delayed development, hypotonia, nystagmus, and extrapyramidal movement disorders (including dystonia, rigidity and, rarely, choreoathetosis) (Hamilton et al., 2014; van der Knaap et al., 2007). The most commonly published *TUBB4A* mutation, c.745G > A, appears to be found in the least severely affected patients; other mutations are associated with earlier onset and an inability to achieve independent ambulation, along with lower likelihood of achieving speech or social awareness (Hamilton et al., 2014). Early MRI (<2 years after onset) shows moderate to severe lack of myelination with a variable degree of putaminal atrophy and moderate cerebellar atrophy. Subsequent studies show slowly progressive loss of myelin, but more rapidly progressive atrophy of putamen (which ultimately completely disappears), caudate, corpus callosum, and cerebellum (Hamilton et al., 2014). It is important to recognize that the degree of basal ganglia and cerebellar atrophy varies among affected patients; indeed, *a recent report describes 5 patients with TUBB4A mutations who have hypomyelination but normal basal ganglia and cerebellum* (Pizzino et al., 2014); therefore, *TUBB4A* mutation screening should be routinely performed in isolated hypomyelination without a known cause.

Trichothiodystrophy with photosensitivity (also called *Tay syndrome* (Østergaard and Christensen, 1996)) is a rare autosomal dominant disease caused by mutations of several different DNA repair genes: *ERCC2* (at chromosome 19q13.32) and *ERCC3* (at chromosome 2q14.3), which encode the two helicase subunits of general transcription/repair factor IIH (TFIIH); and *GTF2H5*, which encodes the tenth subunit of TFIIH (Hoeijmakers, 1994; Weeda et al., 1997; Giglia-Mari et al., 2004; Hashimoto and Egly, 2009). In addition to abnormal brittle, fraying hair, photosensitivity and ichthyotic skin, most affected patients present with developmental delay/intellectual impairment, short stature and craniofacial dysmorphisms such as microcephaly, large ears, or micrognathia (Faghri et al., 2008). Neuroimaging abnormalities are uncommonly reported, but include hypomyelination along with cerebral and cerebellar atrophy (Harreld et al., 2010; Ostergaard and Christensen, 1996; Porto et al., 2000).

Two groups of patients with hypomyelinating disorders have mutations of the multienzyme aminoacyl-tRNA synthetase complex (multisynthetase complex), which consists of the cytoplasmic tRNA synthetases for multiple amino acids and 3 auxiliary proteins (Wolfe et al., 2005). Mutations in the *RARS* gene, coding for cytoplasmic arginyl-tRNA synthetase gene (at chromosome 5q34), have been recently identified as the cause of a hypomyelinating leukodystrophy in 4 patients (Wolf et al., 2014). Mutations of another component of the multisynthetase complex, cytoplasmic aspartyl t-RNA synthetase (*DARS*), causes another disorder called hypomyelination with brain stem and spinal cord involvement and leg spasticity (HBSL) (Taft et al., 2013). Possible roles of the multisynthetase complex in these and other disorders are discussed by Wolfe et al. (Wolf et al., 2014). Three patients with *RARS* mutations presented during the first postnatal year with delayed or stagnated motor development, progressing to spasticity, dystonia, dysarthria, nystagmus, and mild cognitive impairment. The fourth was more severely affected, with microcephaly, severe delay in milestones, feeding problems and achievement of few milestones (Wolf et al., 2014). On MRI, all had findings of severe

hypomyelination on T1 and T2 weighted images, with atrophy noted on patient who was imaged in early adulthood. Ten patients with *DARS* mutations presented in the first year of life with abnormalities of muscle tone and delay or loss of motor milestones; three presented with nystagmus. Over time, all developed progressive spasticity of the legs, four developed mild cognitive impairment and two developed epilepsy (Taft et al., 2013). MRIs of patients with *DARS* mutations show homogeneously abnormal supratentorial white matter consistent with hypomyelination, usually with thinning of the corpus callosum, T2 hyperintensity of the ventral pons, ventral medulla, and inferior cerebellar peduncles in the brain stem, and hyperintensity of the dorsal columns of the spinal cord (Taft et al., 2013).

Many authors classify sialic acid storage diseases, fucosidosis, and Cockayne syndrome as HMDs; others include GM2 gangliosidoses in this category as well (Steenweg et al., 2010). We believe that these disorders have a secondary failure of myelination, resulting from neuronal or astrocytic dysfunction and do not discuss them in this review. However, it is important to remember these disorders when a patient is diagnosed with "hypomyelination" by imaging.

2. Advanced imaging of hypomyelination

Since the earliest days of neonatal MRI imaging, nearly 30 years ago, T1 and T2 weighted spin-echo images have been the primary sequences utilized to evaluate myelination (Barkovich et al., 1988; Dietrich et al., 1988; Holland et al., 1986): over the first two years of life, the white matter of the brain turns progressively brighter on T1 weighted images (shortening of the T1 relaxation time) and progressively darker on T2 weighted images (shortening of the T2 relaxation time) (Fig. 1). These changes progress in the same order as the deposition of myelination, as demonstrated by Flechsig (Flechsig, 1920), Yakovlev and Lecours (Yakovlev and Lecours, 1967) and Kinney et al. (Kinney et al., 1988); therefore, they have been presumed to result from the process of myelination. The pictures of the brain seen on MRI are composed exclusively of signal from the hydrogen protons of water molecules. The different signal intensities are the result of T1 and T2 relaxation processes that are known to result from water motion and interactions; these relaxation processes are affected by the physical structure of the molecule interacting with the water and the chemical environment surrounding the water molecules. The amount of water in a voxel, its mobility, its interaction with large molecules and their functional groups (especially hydrogen binding as with hydroxyl and ketone moieties) and effects of free electrons as from paramagnetic molecules (such as iron) have particularly large effects. Interactions of water with the phospholipid-rich membranes and proteins of myelin and iron-containing oligodendrocytes would be expected to cause significant reduction of T1 and T2 relaxation times (Paus et al., 2001). However, it is likely that the T1 and T2 shortening associated with brain maturation has multiple causes, and the strength of the relative contributions from these causes has never been entirely clear. Do the functional groups of myelin proteins bind free water and, thereby, slow its translation and rotation (a direct effect of myelin)? What is the effect of the binding of the water molecules to functional groups of proteins being formed as a result of the nearly simultaneous maturation of the axons, dendrites, and synapses? How does the simultaneous maturation of microtubule-dependent translation of proteins and neurotransmitters affect the motion of the water molecules that are bound to them? What does the development of blood vessels and the associated increase in local vascularity affect water motion? Why are the changes seen first on T1-weighted images and only later on T2 weighted images: is T1 was more sensitive to the changes in water motion or do the T1 and T2 changes differ in sensitivity to the many aspects of the maturation process? All that is known at this time that disorders that are found on histology to have hypomyelination have

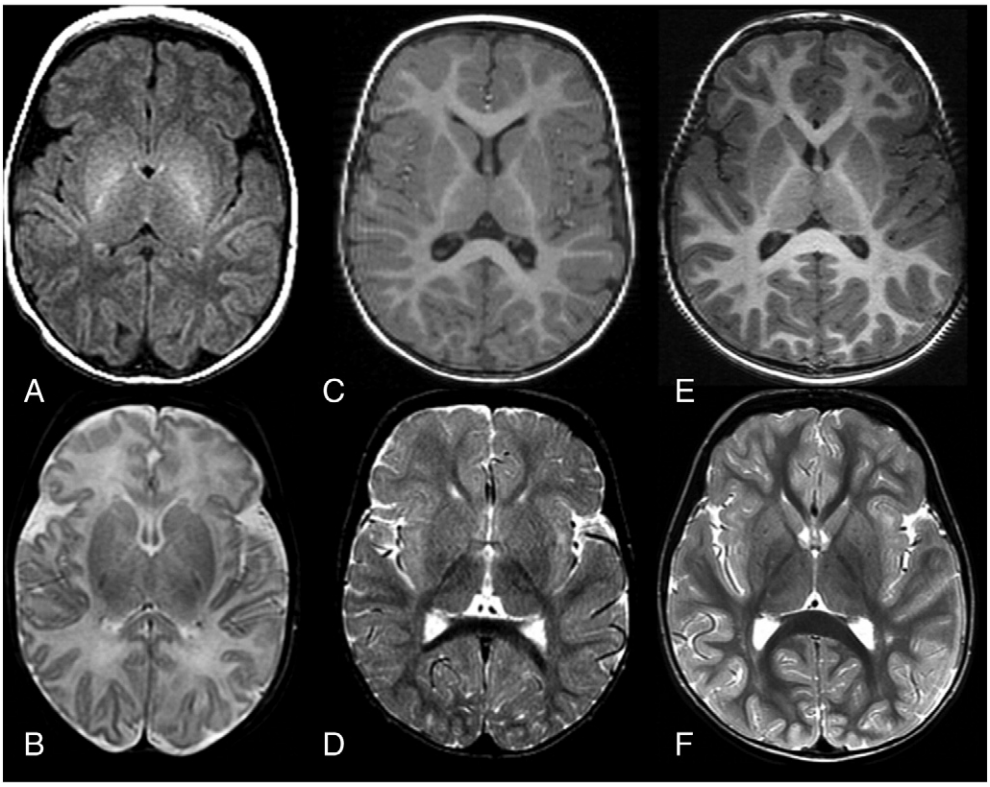

Fig. 1. Normal T1 and T2 changes associated with the process of myelination; T1 weighted images are on top and T2 weighted images on the bottom. A and B show images of a neonate. Note that the white matter is dark compared to cortex and basal ganglia on the T1 image, and the white matter is bright compared to gray matter on the T2 image, except for the posterior limbs of the internal capsules. C and D show images of an 18 month old infant. The white matter has become hyperintense compared to gray matter on the T1 image, but the change has only partially occurred on the T2 weighted image (D), where the frontal white matter is largely isointense to cortex. E and F show that at 34 months, the white matter is fairly uniformly hyperintense compared to gray matter on T1, and fairly uniformly hypointense compared to gray matter on T2.

reduced or delayed T1 and T2 shortening on MRI; this appearance of immaturity should alert the radiologist or clinician to consider hypomyelination as a diagnosis.

Indeed, the diagnosis of HM disorder is usually initially suggested when MRI shows a state of myelination that is *significantly* delayed for the age of the patient compared with normal standards (Barkovich et al., 1988; Paus et al., 2001; Barkovich, 2000; van der Knaap and Valk, 2005c). Occasionally, early illness or prematurity can cause myelination delay; in these situations, a follow-up MRI in 6 months will show normalization or a significant "catching up" of myelination with respect to normal standards. In contrast, MRI of patients with hypomyelination will show little, if any, change in the MRI appearance. In many patients with HM disorders, myelination eventually progresses on MRI, at least transiently, before variably showing myelin loss associated with progressive atrophy of the cerebellum and cerebral white matter (Figs. 2, 3).

While the finding of hypomyelination is nonspecific, the finding of other imaging abnormalities (such as atrophy of the basal ganglia and cerebellum, Fig. 3) can help to narrow the differential diagnosis. The differential diagnosis is often further narrowed after obtaining detailed family history along with developmental history and clinical examination of affected family members. Final diagnosis is made by genetic testing, often using whole exome sequencing.

Advances in stem cell technology have shown potential for stem cell therapy of hypomyelinating disorders (Gupta et al., 2012; Uchida et al., 2012). In a human trial, quantitative diffusion MRI in a small cohort of children with Pelizaeus-Merzbacher disease showed changes (increased fractional anisotropy and reduced radial diffusivity) after stem cell therapy that suggested myelination; a nearly simultaneous trial of stem cell implantation in hypomyelinating mice were subsequently proved to be associated with new myelination in the mice (Gupta et al., 2012; Uchida et al., 2012). Other techniques that have been useful in assessing myelination in animal models include proton MR spectroscopy (Takanashi et al., 2002, 2012; J-i et al., 2013) and magnetization transfer MRI (Dreha-Kulaczewski et al., 2012). These techniques and their potentials will be briefly discussed.

2.1. Magnetization transfer imaging

Magnetization transfer (MT) imaging evaluates magnetization exchange between water protons bound to immobile macromolecules, such as the large proteins and the lipid bilayers of myelin, and unbound protons of free water. This technique involves applying a narrow frequency RF pulse to selectively saturate the bound pool protons but not those in the free water compartment (Wolff and Balaban, 1989). Quantification in the form of magnetization transfer ratio (MTR) is achieved by calculating $MTR = (M_0 - M_{SAT})/M_0$ where M_0 is the magnetization of the liquid (free) water pool (in the absence of exchange between water protons and those of protons bound to myelin) and M_{SAT} is the magnetization of water molecules in the liquid pool exchanging with those in the macromolecular (bound water) pool (Graham and Henkelman, 1999; Henkelman et al., 2001). Studies have revealed that the MT characteristics of cerebral white matter are caused

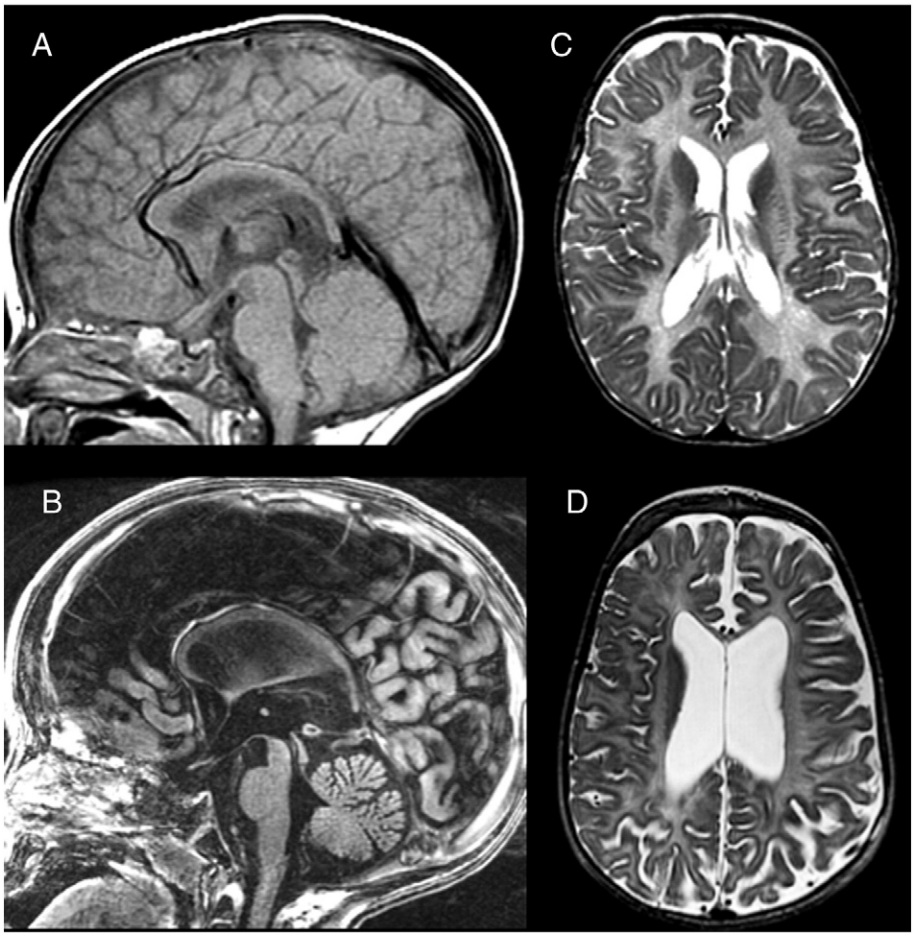

Fig. 2. Pelizaeus–Merzbacher Disease. T1 sagittal (A) and T2 axial (C) images obtained at age 7 months for nystagmus show a normal midline in (A) but significant hypomyelination, which is more obvious in (C). Follow-up images at age 28 months (B, D) due to clinical deterioration show development of significant atrophy, both supra- and infratentorially. No significant myelination has developed.

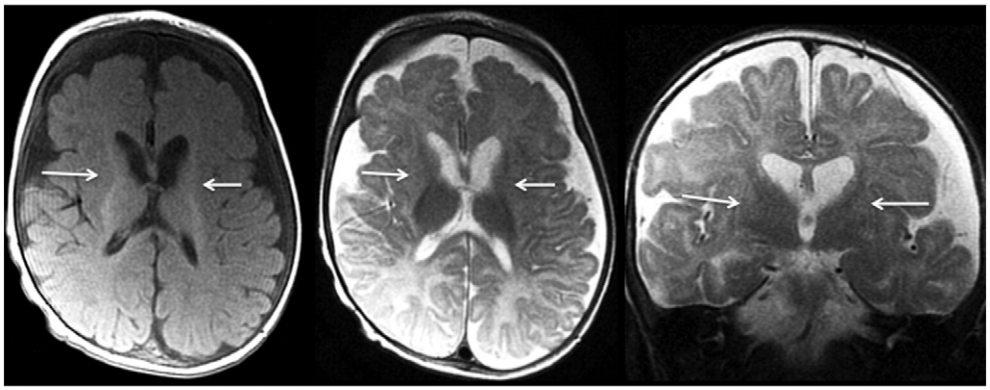

Fig. 3. Hypomyelination with atrophy of the basal ganglia and cerebellum (HABC) in a hypotonic, 8 month old boy with dystonia and contractures. Axial T1 left) and axial center) and coronal right) T2-weighted images show insufficient myelination for age. Notice that the lateral walls of the frontal horns are insufficiently convex because the caudate heads are atrophic and the putamina (arrows) are barely visible.

primarily by myelin (Stanisz et al., 1999). Reproducibility of MT data appears to be better than that of myelin water fraction imaging (see below) (Dula et al., 2010).

MT MRI imaging shows that T1 and T2 imaging changes linearly correlate with the amount of MT (Dreha-Kulaczewski et al., 2012; Sled and Pike, 2001) (Fig. 4). Moreover, MT methods can be quantified through

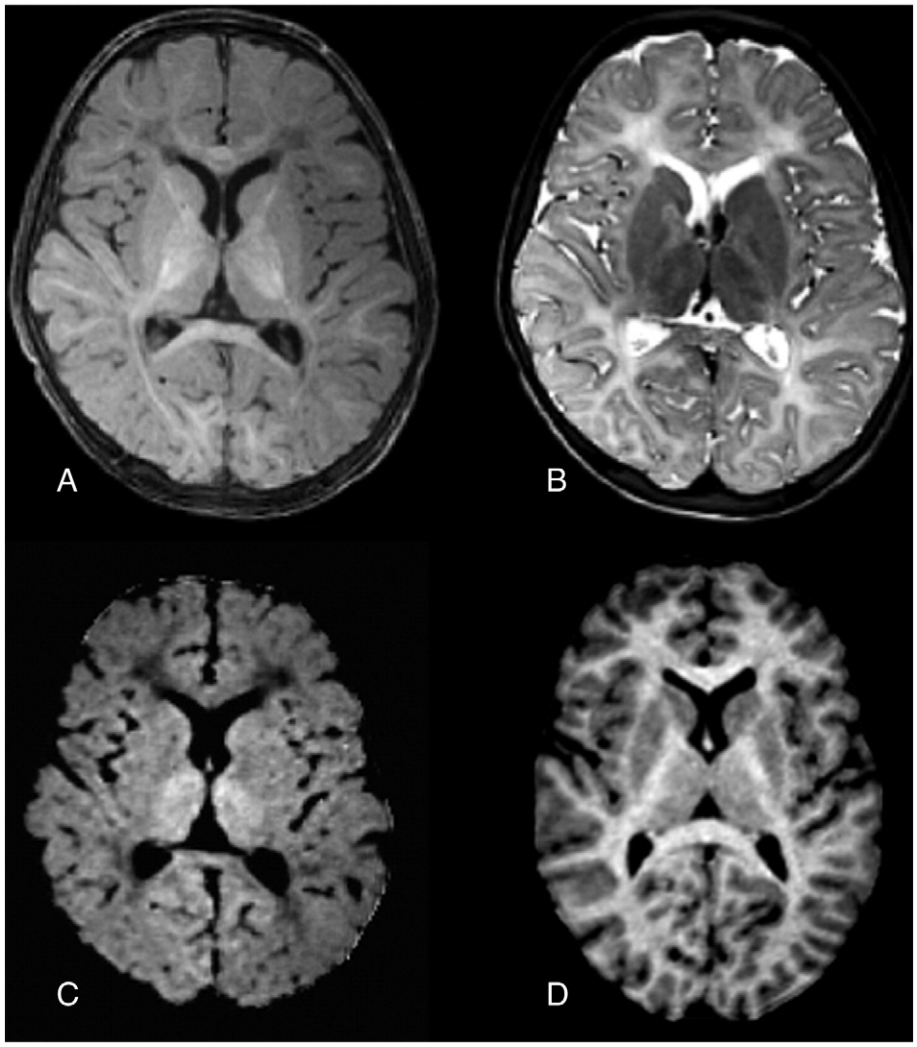

Fig. 4. Leukodystrophy due to *POL3A* mutation (4H syndrome) in a 4.5 year old boy. Axial T1 (A) and T2 (B) weighted images show profoundly delayed myelination with some T1 shortening (hyperintensity) in the internal capsules, lateral thalami, optic radiations and corpus callosum (A), but virtually no T2 changes of myelination (B). A magnetization transfer image (C) shows evidence of essentially no magnetization transfer, which would appear as hyperintensity of white matter, as in the age matched control image (D). The amount of magnetization transfer can be quantified, and is used by some as a quantitative marker of myelination.
(These images courtesy of Dr. Steffi Dreha-Kulaczewski, University Medical Center Göttingen, Germany).

the used of complex modeling of the liquid and bound pools (see section on Myelin Water Fraction below) (Sled and Pike, 2001; Levesque and Pike, 2009). Studies of animal models of demyelination have shown that bound pool fraction and the MTR correlate well with the quantity of myelin, but also with the presence of other membranes (in axons and glia) (Bjarnson et al., 2005; Blezer et al., 2007; Odrobina et al., 2005; Schmierer et al., 2007), suggesting (Schiffmann and van der Knaap, 2009) that MT imaging is sensitive but not specific in the assessment of myelination, but also (Steenweg et al., 2010) that it may assess myelin *development* more accurately than inflammatory *demyelination* because quantification of the latter would be altered by the effects of the associated inflammatory cells. Indeed, quantitative MT imaging has been proven useful in quantifying brain maturation (both myelination and other aspects of development) in normal development (Nossin-Manor et al., 2012, 2013) and in hypomyelinating disorders (Dreha-Kulaczewski et al., 2012). Thus, MT imaging has strong potential for quantifying myelination in patients with HMDs and in assessing the efficacy of treatments.

2.2. Myelin water fraction

Quantitative T1 and T2 weighted imaging has been used in an attempt to make MRI relaxometry (increasing T1 hyperintensity and T2 hypointensity) more specific. The most useful approach is the multiple component, myelin water fraction (MWF) method, which assumes that T1 and T2 signal curves seen in imaging voxels are a mixture of signals from several distinct tissue environments that have different T1 and T2 characteristics resulting from the unique microstructure(s) that the water protons encounter in these different environments during the image acquisition (Mackay et al., 1994; Menon et al., 1991). Multiple component analysis is used to separate and quantify each component of T1 and T2 relaxation in order to better understand and quantify the contribution of myelin. This can be accomplished by acquiring spin echo relaxation data using a wide range of repetition (TR) and echo (TE) times (Whittall et al., 1997; Labadie et al., 2014). Using a least squares approach to fit a semicontinuous log T1 or T2 distribution to the sampled data, a bi- or *trimodal profile* is revealed: (Schiffmann and van der Knaap, 2009) a short T1 or T2 peak attributed to water trapped between myelin bilayers; (Steenweg et al., 2010) a peak with intermediate T1 or T2 relaxation time attributed to intracellular and extracellular water; and (Schiffmann et al., 1994) a long T1 or T2 peak attributed to CSF (Labadie et al., 2014; MacKay et al., 2006). The MWF is defined by the ratio of the area under the short T1 or T2 peak to the area under the total T1 or T2 distribution, respectively. This method has been shown to correlate strongly with assessments of myelin by histology (Whittall et al., 1997; MacKay et al., 2006; Gareau et al., 2000). Unfortunately, the utility of MWF imaging has been hampered to date by lengthy acquisition times; new approaches using new techniques such as mcDESPOT may make this method more feasible (Deoni and Kolind, 2015), but questions regarding the specificity of this technique remain (Lankford and Does, 2013).

2.3. Diffusion imaging

In diffusion tensor imaging (DTI), strong gradient pulses are applies to a sample in order to assess the direction and magnitude of water motion in tissue. The major parameters measured are: (Schiffmann and van der Knaap, 2009) *fractional anisotropy* (FA), assessing the degree of parallel motion of water molecules; (Steenweg et al., 2010) radial diffusivity (RD), assessing motion perpendicular to the axon; and (Schiffmann et al., 1994) axial diffusivity (AD), assessing motion parallel to the axon. FA = 1 is defined as the (theoretical) state where all water molecules move in parallel, while FA = 0 is defined as that state where all water motion is completely random. As myelin is hydrophobic and enlarges the effective diameter of the axon, myelination would be expected to increase FA, reduce RD, and have little effect upon AD (Dubois et al., 2006, 2014; Vasung et al., 2013). Experiments in mouse models of hypomyelination have supported these concepts, with the RD changes being the largest (Harsan et al., 2006; Ruest et al., 2011; Song et al., 2002). The accuracy of information can be increased by the use of advanced diffusion imaging techniques: high angular resolution diffusion imaging (HARDI) with multiple b values are optimal, but these require strong magnetic fields and rather long examination times (Jones et al., 2013).

The ultimate goal of diffusion imaging is to be able to quantify myelin formation based upon FA and RD values. Progress has been made. Increases in RD have been shown to correspond to reversible hypomyelination in *hsv-tk1* mouse models (Harsan et al., 2006). *Shi* mice transplanted with human neural stem cells showed increased FA, and human subjects with PMD showed decreased RD and increased FA after transplantation with human neural stem cells (Pouwels et al., 2014). Overall, however, the quantification of myelination has not been successful. Among the many reasons for this are the size of the voxels used in human imaging, which are many orders of magnitude larger than the size of the axons (Pierpaoli and Basser, 1996), perturbations of water motion by brain many structures other than myelin (Hüppi et al., 1998; Prayer et al., 2001; Wimberger et al., 1995), and the non-Gaussian distribution of water motion (DTI assumes a Gaussian distribution). Although the latter issue can be addressed by use of diffusion kurtosis imaging (Jensen and Helpern, 2010), the other issues are significantly more difficult to address. Nonetheless, although processes other than myelination affect water motion, myelin is likely the most dominant effect in patients beyond the first few months of life; therefore, results from diffusion techniques, together with magnetization transfer, are fairly specific techniques for its quantification and will almost certainly get better.

2.4. Proton MR spectroscopy

Proton MR spectroscopy (MRS) is an analytical tool that has been used for many decades in analytical chemistry to determine the structure of molecules based mainly on analysis of the influence of surrounding electrons upon the magnetic field that is felt by each proton in the molecule being investigated (chemical shift) and the effect of neighboring nuclei on splitting of the peak (spin–spin coupling). These two factors give each molecular compound a specific NMR fingerprint. Moreover, the area under the MRS peak gives the concentration of the compound, allowing quantitative assessment of molecular concentrations (Barker, 2010; Ernst, 2010). Unfortunately, many protons in biologically important chemicals cannot be seen on in vivo MRS because they have T2 relaxation times that are too short or concentrations too low to allow them to be analyzed by MRI machines that are used for medical diagnoses. Analyses are, therefore, limited to the few chemical compounds that can be adequately assessed: N-acetylaspartate (NAA), glutamate, glutamine, succinate, aspartate, creatine, choline, lactate, glycine, branched chain amino acids and myo-inositol. Unfortunately, these compounds are not specific for myelin and their size does not give any direct information regarding the quantity of myelin in the areas being sampled.

In vivo MRS of myelin is complicated by the complexity of myelin structure, with its many protein and lipid components and by the very short T2 relaxation times of many of the protons being investigated (Wilhelm et al., 2012). MRS of myelin, as a result, gives a broad peak that overlaps with peaks from other membranes and, therefore, relies almost solely upon the T2 relaxation time (actually $T2^*$ relaxation time (Wilhelm et al., 2012)) for identification; this makes in vivo identification by MRI machines very difficult and, even if possible, could lead to other compounds being falsely identified as myelin (Wilhelm et al., 2012).

Studies of patients with HMDs and animal models of HMDs, however, have shown some characteristic findings. Patients with the classic form of PMD have abnormally large NAA and NAAG peaks (Takanashi

et al., 2002; Hanefeld et al., 2005). This likely results from an unfolded protein response triggered by the abnormal proteolipid protein moieties that accumulate in the endoplasmic reticulum in these patients; injury/apoptotic death of oligodendrocytes ensues (Dhaunchak et al., 2011). As NAA is metabolized to acetate and aspartate in oligodendrocytes (Benarroch, 2008), their loss results causes accumulation of NAA and its elevated concentration results in an increased amount being converted to NAAG, which has a nearly identical chemical shift (Barker, 2010) and results in a visible increase in "total NAA" (Takanashi et al., 2012). Analysis by high pressure liquid chromatography in the *msd* mouse showed the presence of both increased NAA and NAAG, strongly supporting this theory (Takanashi et al., 2012).

In summary, although judicious use of MRS is useful in helping the understanding of some hypomyelinating disorders, and the demonstration of an enlarged NAA/NAAG peak can be helpful to diagnose PMD, MRS seems unlikely to provide additional diagnostic information or to help to quantify myelination in the near future.

3. Conclusion

Hypomyelinating disorders are a heterogeneous group of diseases affecting the developing brain and, often, other organs as well. They are considered as a group because nearly all are referred for MRI due to their nearly ubiquitous neurological and/or developmental disorder. The uncommon finding of hypomyelination, if recognized, can markedly reduce the time and expense of the metabolic work-up. Understanding these disorders can aid in counseling patients and their families and, perhaps, developing and testing therapies.

References

Barker, P.B., 2010. Fundamentals of MR spectroscopy. In: Gillard, J.H., Waldman, A.D., Barker, P.B. (Eds.), Clinical MR Imaging, 2nd ed. Cambridge, New York, pp. 5–20.

Barkovich, A.J., 2000. Concepts of myelin and myelination in neuroradiology. AJNR Am. J. Neuroradiol. 21 (6), 1099–1109.

Barkovich, A.J., Kjos, B.O., Jackson Jr., D.E., Norman, D., 1988. Normal maturation of the neonatal and infant brain: MR imaging at 1.5 T. Radiology 166, 173–180.

Benarroch, E.E., 2008. N-acetylaspartate and N-acetylaspartylglutamate. Neurobiology and clinical significance. Neurology 70, 1353–1357.

Bernard, G., Vanderver, A., 2012. Pol III-related leukodystrophies. Gene Rev. (http://www.ncbi.nlm.nih.gov/pubmed/22855961).

Biancheri, R., Zara, F., Bruno, C., et al., 2007. Phenotypic characterization of hypomyelination and congenital cataract. Ann. Neurol. 62, 121–127.

Biancheri, R., Zara, F., Rossi, A., et al., 2011. Hypomyelination and congenital cataract: broadening the clinical phenotype. Arch. Neurol. 68 (9), 1191–1194.

Biancheri, R., Rosano, C., Denegri, L., et al., 2013. Expanded spectrum of Pelizaeus–Merzbacher-like disease: literature revision and description of a novel GJC2 mutation in an unusually severe form. Eur. J. Hum. Genet. 21, 34–39.

Bjarnson, T.A., Vavasour, I.M., Chia, C.L.L., MacKay, A.L., 2005. Characterization of the NMR behaviour of white matter in bovine brain. Magn. Reson. Med. 54, 1072–1081.

Blezer, E.L.A., Bauer, J., Brok, H.P.M., Nicolay, K., 2007. t Hart BA. Quantitative MRI-pathology correlations of brain white matter lesions developing in a non-human primate model of multiple sclerosis. NMR Biomed. 20 (2), 90–103.

Boespflug-tanguy, O., 2013. Chapter 162 — inborn errors of brain myelin formation. In: Olivier Dulac, M.L., Harvey, B.S. (Eds.), Handbook of Clinical Neurology vol. 113. Elsevier, pp. 1581–1592.

Daoud, H., Tétreault, M., Gibson, W., et al., 2013. Mutations in POLR3A and POLR3B are a major cause of hypomyelinating leukodystrophies with or without dental abnormalities and/or hypogonadotropic hypogonadism. J. Med. Genet. 50 (3), 194–197 (March 1, 2013).

De Bock, M., Kerrebrouck, M., Wang, N., Leybaert, L., 2013. Neurological manifestations of oculodentodigital dysplasia: a Cx43 channelopathy of the central nervous system? Front. Pharmacol. 4.

Deoni, S.C.L., Kolind, S.H., 2015. Investigating the stability of mcDESPOT myelin water fraction values derived using a stochastic region contraction approach. Magn. Reson. Med. 73 (1), 161–169.

Dhaunchak, A.S., Colman, D.R., Nave, K.-A., 2011. Misalignment of PLP/DM20 transmembrane domains determines protein misfolding in Pelizaeus–Merzbacher disease. J. Neurosci 31 (42), 14961–14971.

Dietrich, R.B., Bradley, W.G., Zagaroza, E.J., et al., 1988. MR evaluation of early myelination patterns in normal and developmentally delayed infants. AJNR Am. J. Neuroradiol. 9, 69–76.

Dreha-Kulaczewski, S.F., Brockmann, K., Henneke, M., et al., 2012. Assessment of myelination in hypomyelinating disorders by quantitative MRI. J. Magn. Reson. Imaging (n/a-n/a).

Dubois, J., Hertz-Pannier, L., Dehaene-Lambertz, G., Cointepas, Y., Le Bihan, D., 2006. Assessment of the early organization and maturation of infants' cerebral white matter fiber bundles: a feasibility study using quantitative diffusion tensor imaging and tractography. NeuroImage 30, 1121–1132.

Dubois, J., Dehaene-Lambertz, G., Kulikova, S., Poupon, C., Hüppi, P.S., Hertz-Pannier, L., 2014. The early development of brain white matter: a review of imaging studies in fetuses, newborns and infants. Neuroscience 276, 48–71.

Dula, A.N., Gochberg, D.F., Valentine, H.L., Valentine, W.M., Does, M.D., 2010. Multiexponential T2, magnetization transfer, and quantitative histology in white matter tracts of rat spinal cord. Magn. Reson. Med. 63 (4), 902–909.

Ernst, T., 2010. Quantification and analysis in MR spectroscopy. In: Gillard, J.H., Waldman, A.D., Barker, P.B. (Eds.), Clinical MR Imaging, 2nd ed. Cambridge, New York, pp. 21–29.

Etienne-Manneville, S., 2013. Microtubules in cell migration. Annu. Rev. Cell Dev. Biol. 29, 471–499.

Faghri, S., Tamura, D., Kraemer, K.H., DiGiovanna, J.J., 2008. Trichothiodystrophy: a systematic review of 112 published cases characterises a wide spectrum of clinical manifestations. J. Med. Genet. 45 (10), 609–621 (October 1, 2008).

Flechsig, P., 1920. Anatomie des menschlichen Gehirns und Ruchenmarks auf myelogenetischer Grundlage. Georg Thieme, Leipzig.

Franker, M.A.M., Hoogenraad, C.C., 2013. Microtubule-based transport — basic mechanisms, traffic rules and role in neurological pathogenesis. J. Cell Sci. 126 (11), 2319–2329 (June 1, 2013).

Garbern, J.Y., Cambi, F., Lewis, R., et al., 1999. Peripheral neuropathy caused by proteolipid protein gene mutations. Ann. N. Y. Acad. Sci. 883 (1), 351–365.

Gareau, P.J., Rutt, B.K., Karlik, S.J., Mitchell, J.R., 2000. Magnetization transfer and multicomponent T2 relaxation measurements with histopathologic correlation in an experimental model of MS. J. Magn. Reson. Imaging 11 (6), 586–595.

Giglia-Mari, G., Coin, F., Ranish, J.A., et al., 2004. A new, tenth subunit of TFIIH is responsible for the DNA repair syndrome trichothiodystrophy group A. Nat. Genet. 36 (7), 714–719 (07//print).

Gotoh, L., Inoue, K., Helman, G., et al., 2014. GJC2 promoter mutations causing Pelizaeus–Merzbacher-like disease. Mol. Genet. Metab. 111 (3), 393–398 (3//).

Graham, S.J., Henkelman, R.M., 1999. Pulsed magnetization transfer imaging: evaluation of technique. Radiology 212 (3), 903–910 (1999/09/01).

Gupta, N., Henry, R.G., Strober, J., et al., 2012. Neural stem cell engraftment and myelination in the human brain. Sci. Transl. Med. 4 (155), 155ra137 (October 10, 2012).

Gutmann, D., Zackai, E., McDonald-McGinn, D., Fischbeck, K., Kamholz, J., 1991. Oculodentodigital dysplasia syndrome associated with abnormal cerebral white matter. Am. J. Med. Genet. 41, 18–20.

Gv, B., Chouery, E., Putorti, M.L., et al., 2011. Mutations of POLR3A encoding a catalytic subunit of RNA polymerase Pol III cause a recessive hypomyelinating leukodystrophy. Am. J. Hum. Genet. 89 (3), 415–423.

Hamilton, E.M., Polder, E., Vanderver, A., et al., 2014. Hypomyelination with atrophy of the basal ganglia and cerebellum: further delineation of the phenotype and genotype–phenotype correlation. Brain 137 (7), 1921–1930.

Hanefeld, F.A., Brockmann, K., Pouwels, P.J.W., Wilken, B., Frahm, J., Dechent, P., 2005. Quantitative proton MRS of Pelizaeus–Merzbacher disease. Evidence of dys- and hypomyelination. Neurology 65, 701–706.

Harreld, J.H., Smith, E.C., Prose, N.S., Puri, P.K., Barboriak, D.P., 2010. Trichothiodystrophy with dysmyelination and central osteosclerosis. AJNR Am. J. Neuroradiol. 31, 129–130.

Harsan, L.A., Poulet, P., Guignard, B., et al., 2006. Brain dysmyelination and recovery assessment by noninvasive in vivo diffusion tensor magnetic resonance imaging. J. Neurosci. Res. 83 (3), 392–402.

Hashimoto, S., Egly, J.M., 2009. Trichothiodystrophy view from the molecular basis of DNA repair/transcription factor TFIIH. Hum. Mol. Genet. 18 (R2), R224–R230 (October 15, 2009).

Henkelman, R.M., Stanisz, G.J., Graham, S.J., 2001. Magnetization transfer in MRI: a review. NMR Biomed. 14 (2), 57–64.

Hoeijmakers, J.H.J., 1994. Human nucleotide excision repair syndromes: molecular clues to unexpected intricacies. Cancer 30A, 1912–1924.

Holland, B.A., Haas, D.K., Norman, D., Brant-Zawadzki, M., Newton, T.H., 1986. MRI of normal brain maturation. Am. J. Neuroradiol. 7, 201–208.

Hüppi, P., Maier, S., Peled, S., et al., 1998. Microstructural development of human newborn cerebral white matter assessed in vivo by diffusion tensor magnetic resonance imaging. Pediatr. Res. 44, 584–590.

Jensen, J.H., Helpern, J.A., 2010. MRI quantification of non-Gaussian water diffusion by kurtosis analysis. NMR Biomed. 23 (7), 698–710.

J-i, T., Nitta, N., Iwasaki, N., et al., 2013. Neurochemistry in shiverer mouse depicted on MR spectroscopy. J. Magn. Reson. Imaging (n/a-n/a).

Jones, D.K., Knösche, T.R., Turner, R., 2013. White matter integrity, fiber count, and other fallacies: the do's and don'ts of diffusion MRI. NeuroImage 73 (0), 239–254 (6//).

Kevelam, S.H., Taube, J.R., van Spaendonk, R.M.L., et al., 2015. Altered PLP1 splicing causes hypomyelination of early myelinating structures. Ann. Clin. Transl. Neurol. 2 (6), 648–661.

Kinney, H.C., Brody, B.A., Kloman, A.S., Gilles, F.H., 1988. Sequence of central nervous system myelination in human infancy. II. Patterns of myelination in autopsied infants. J. Neuropathol. Exp. Neurol. 47, 217–234.

Koeppen, A.H., Ronca, N.A., Greenfield, E., Hans, M.B., 1987. Defective biosynthesis of proteolipid protein in Pelizaeus–Merzbacher disease. Ann. Neurol. 21, 159–170.

La Piana, R., Tonduti, D., Dressman, H.G., et al., 2014. Brain magnetic resonance imaging (MRI) pattern recognition in Pol III-related leukodystrophies. J. Child Neurol. 29 (2), 214–220 February 1, 2014.

Labadie, C., Lee, J.-H., Rooney, W.D., et al., 2014. Myelin water mapping by spatially regularized longitudinal relaxographic imaging at high magnetic fields. Magn. Reson. Med. 71 (1), 375–387.

Lankford, C.L., Does, M.D., 2013. On the inherent precision of mcDESPOT. Magn. Reson. Med. 69 (1), 127–136 03/12.
Levesque, I.R., Pike, G.B., 2009. Characterizing healthy and diseased white matter using quantitative magnetization transfer and multicomponent T2 relaxometry: a unified view via a four-pool model. Magn. Reson. Med. 62 (6), 1487–1496.
LeVine, S.M., Wong, D., Macklin, W.B., 1990. Developmental expression of proteolipid protein and DM20 mRNAs and proteins in the rat brain. Dev. Neurosci. 12 (4–5), 235–250.
Linnankivi, T., Tienari, P., Somer, M., et al., 2006. 18q deletions: clinical, molecular, and brain MRI findings of 14 individuals. Am. J. Med. Genet. A 140A (4), 331–339.
Mackay, A., Whittall, K., Adler, J., Li, D., Paty, D., Graeb, D., 1994. In vivo visualization of myelin water in brain by magnetic resonance. Magn. Reson. Med. 31 (6), 673–677.
MacKay, A., Laule, C., Vavasour, I., Bjarnason, T., Kolind, S., Mädler, B., 2006. Insights into brain microstructure from the T2 distribution. Magn. Reson. Imaging 24 (4), 515–525 (5//).
Menichella, D.M., Goodenough, D.A., Sirkowski, E., Scherer, S.S., Paul, D.L., 2003. Connexins are critical for normal myelination in the CNS. J. Neurosci. 23 (13), 5963–5973 (July 2, 2003).
Menon, R.S., Rusinko, M.S., Allen, P.S., 1991. Multiexponential proton relaxation in model cellular systems. Magn. Reson. Med. 20 (2), 196–213.
Meyer, E., Kurian, M.A., Morgan, N.V., et al., 2011. Promoter mutation is a common variant in GJC2-associated Pelizaeus–Merzbacher-like disease. Mol. Genet. Metab. 104 (4), 637–643.
Norton, K., Carey, J.C., Gutmann, D.H., 1995. Oculodentodigital dysplasia with cerebral white matter abnormalities in a two-generation family. Am. J. Med. Genet. 57, 458–461.
Nossin-Manor, R., Chung, A.D., Whyte, H.E.A., Shroff, M.M., Taylor, M.J., Sled, J.G., 2012. Deep gray matter maturation in very preterm neonates: regional variations and pathology-related age-dependent changes in magnetization transfer ratio. Radiology 263 (2), 510–517 (2012/05/01).
Nossin-Manor, R., Card, D., Morris, D., et al., 2013. Quantitative MRI in the very preterm brain: assessing tissue organization and myelination using magnetization transfer, diffusion tensor and T1 imaging. NeuroImage 64 (0), 505–516 (1/1/).
Numata, Y., Morimura, T., Nakamura, S., et al., 2013. Depletion of molecular chaperones from the endoplasmic reticulum and fragmentation of the Golgi apparatus associated with pathogenesis in Pelizaeus–Merzbacher disease. J. Biol. Chem. 288 (11)), 7451–7466 March 15, 2013.
Odrobina, E.E., Lam, T.Y.J., Pun, T., Midha, R., Stanisz, G.J., 2005. MR properties of excised neural tissue following experimentally induced demyelination. NMR Biomed. 18 (5), 277–284.
Ostergaard, J.R., Christensen, T., 1996. The central nervous system in Tay syndrome. Neuropediatrics 27, 326–330.
Østergaard, J.R., Christensen, T., 1996. The central nervous system in Tay syndrome. Neuropediatrics 27, 326–330.
Paus, T., Collins, D.L., Evans, A.C., Leonard, G., Pike, B., Zijdenbos, A., 2001. Maturation of white matter in the human brain: a review of magnetic resonance studies. Brain Res. Bull. 54 (3), 255–266 (2//).
Paznekas, W.A., Karczeski, B., Vermeer, S., et al., 2009. GJA1 mutations, variants, and connexin 43 dysfunction as it relates to the oculodentodigital dysplasia phenotype. Hum. Mutat. 30 (5), 724–733.
Pierpaoli, C., Basser, P.J., 1996. Toward a quantitative assessment of diffusion anisotropy. Magn. Reson. Med. 36 (6), 893–906.
Pizzino, A., Pierson, T.M., Guo, Y., et al., 2014. TUBB4A de novo mutations cause isolated hypomyelination. Neurology 83 (10), 898–902 (02/07/received 06/02/accepted).
Porto, L., Weis, R., Schulz, C., Reichel, P., Lanfermann, H., Zanella, F.E., 2000. Tay's syndrome: MRI. Neuroradiology 42, 849–851.
Pouwels, P.J.W., Vanderver, A., Bernard, G., et al., 2014. Hypomyelinating leukodystrophies: translational research progress and prospects. Ann. Neurol. 76 (1), 5–19.
Prayer, D., Barkovich, A.J., Kirschner, D.A., et al., 2001. Visualization of nonstructural changes in early white matter development on diffusion weighted MR images: evidence supporting premyelination anisotropy. AJNR Am. J. Neuroradiol. 22, 1572–1576.
Ruest, T., Holmes, W.M., Barrie, J.A., et al., 2011. High-resolution diffusion tensor imaging of fixed brain in a mouse model of Pelizaeus–Merzbacher disease: comparison with quantitative measures of white matter pathology. NMR Biomed. 24, 1369–1379.
Sakakibara, A., Ando, R., Sapir, T., Tanaka, T., 2013. Microtubule dynamics in neuronal morphogenesis. Open Biol. 3 (7).
Schiffmann, R., van der Knaap, M.S., 2009. Invited article: an MRI-based approach to the diagnosis of white matter disorders. Neurology 72 (8), 750–759.
Schiffmann, R., Moller, J.R., Trapp, B.D., et al., 1994. Childhood ataxia with diffuse central nervous system hypomyelination. Ann. Neurol. 35, 331–340.
Schmierer, K., Tozer, D.J., Scaravilli, F., et al., 2007. Quantitative magnetization transfer imaging in postmortem multiple sclerosis brain. J. Magn. Reson. Imaging 26 (1), 41–51.
Simons, C., Wolf Nicole, I., McNeil, N., et al., 2013. A de novo mutation in the β-tubulin gene TUBB4A results in the leukoencephalopathy hypomyelination with atrophy of the basal ganglia and cerebellum. Am. J. Hum. Genet. (0).
Sistermans, E.A., de Coo, rFM., De Wijs, I.J., Van Oost, B.A., 1998. Duplication of the proteolipid protein gene is the major cause of Pelizaeus–Merzbacher disease. Neurology 50, 1749–1754.
Sled, J.G., Pike, G.B., 2001. Quantitative imaging of magnetization transfer exchange and relaxation properties in vivo using MRI. Magn. Reson. Med. 46 (5), 923–931.
Song, S.-K., Sun, S.-W., Ramsbottom, M.J., Chang, C., Russell, J., Cross, A.H., 2002. Dysmyelination revealed through MRI as increased radial (but unchanged axial) diffusion of water. NeuroImage 17 (3), 1429.
Southwood, C.M., Garbern, J.Y., Jiang, W., Gow, A., 2002. The unfolded protein response modulates disease severity in Pelizaeus–Merzbacher disease. Neuron 36 (4), 585–596.
Stanisz, G.J., Kecojevic, A., Bronskill, M.J., Henkelman, R.M., 1999. Characterizing white matter with magnetization transfer and T2. Magn. Reson. Med. 42 (6), 1128–1136.
Steenweg, M., Vanderver, A., Blaser, S., et al., 2010. Magnetic resonance imaging pattern recognition in hypomyelinating disorders. Brain 133, 2971–2982.
Tada, H., Takanashi, J.-i., 2014. MR spectroscopy in 18q-syndrome suggesting other than hypomyelination. Brain Dev. 36 (1), 57–60 (1//).
Taft, R., Vanderver, A., Leventer Richard, J., et al., 2013. Mutations in DARS cause hypomyelination with brain stem and spinal cord involvement and leg spasticity. Am. J. Hum. Genet. 92 (5), 774–780.
Takanashi, J., Inoue, K., Tomita, M., et al., 2002. Brain N-acetylaspartate is elevated in Pelizaeus–Merzbacher disease with PLP1 duplication. Neurology 58, 237–241.
Takanashi, J., Saito, S., Aoki, I., Barkovich, A.J., Ito, Y., Inoue, K., 2012. Increased N-acetylaspartate in mouse model of Pelizaeus–Merzbacher disease. J. Magn. Reson. Imaging 35, 418–425.
Tanaka, R., Iwasaki, N., Hayashi, M., et al., 2012. Abnormal brain MRI signal in 18q-syndrome not due to dysmyelination. Brain Dev. 34 (3), 234–237.
Traverso, M., Assereto, S., Gazzerro, E., et al., 2013. Novel FAM126A mutations in hypomyelination and congenital cataract disease. Biochem. Biophys. Res. Commun. 439 (3), 369–372 (9/27/).
Uchida, N., Chen, K., Dohse, M., et al., 2012. Human neural stem cells induce functional myelination in mice with severe dysmyelination. Sci. Transl. Med. 4 (155), 155ra136 (October 10, 2012).
Ugur, S.A., Tolun, A., 2008. A deletion in DRCTNNB1A associated with hypomyelination and juvenile onset cataract. Eur. J. Hum. Genet. 16, 261–264.
Uhlenberg, B., Schuelke, M., Rüschendorf, F., et al., 2004. Mutations in the gene encoding gap junction protein alpha-12 (Connexin 46.6) cause Pelizaeus–Merzbacher-like disease. Am. J. Hum. Genet. 75 (2), 251–260.
van der Knaap, M.S., Valk, J., 2005a. Pelizaeus Merzbacher disease and X-linked spastic paraplegia type 2. In: van der Knaap, M.S., Valk, J. (Eds.), Magnetic Resonance of Myelin, Myelination, and Myelin Disorders, 3rd ed. Springer, Berlin, pp. 272–280.
van der Knaap, M.S., Valk, J., 2005b. 18q-syndrome. In: van der Knaap, M.S., Valk, J. (Eds.), Magnetic Resonance of Myelination and Myelin Disorders, 3rd ed. Springer, Berlin, pp. 281–283.
van der Knaap, M.S., Valk, J., 2005c. Magnetic Resonance of Myelination and Myelin Disorders, 3rd Edition. 3rd ed. Springer, Berlin.
van der Knaap, M., Linnankivi, T., Paetau, A., et al., 2007. Hypomyelination with atrophy of the basal ganglia and cerebellum: follow-up and pathology. Neurology 69, 166–171.
Vasung, L., Fischi-Gomez, E., Hüppi, P., 2013. Multimodality evaluation of the pediatric brain: DTI and its competitors. Pediatr. Radiol. 43 (1), 60–68 (2013/01/01).
Walczak, C.E., Gayek, S., Ohi, R., 2013. Microtubule-depolymerizing kinesins. Annu. Rev. Cell Dev. Biol. 29 (1), 417–441 (2013/10/06).
Weeda, G., Eveno, E., Donker, I., et al., 1997. A mutation in the XPB/ERCC3 DNA repair transcription gene, associated with trichothiodystrophy. Am. J. Hum. Genet. 60, 320–329.
Whittall, K.P., MacKay, A.L., Graeb, D.A., Nugent, R.A., Li, D.K., Paty, D.W., 1997. In vivo measurement of T2 distributions and water contents in normal human brain. Magn. Reson. Med. 40, 34–43.
Wilhelm, M.J., Ong, H.H., Wehrli, S.L., et al., 2012. Direct magnetic resonance detection of myelin and prospects for quantitative imaging of myelin density. Proc. Natl. Acad. Sci. 109 (24), 9605–9610 (June 12, 2012).
Wimberger, D.M., Roberts, T.P., Barkovich, A.J., Prayer, L.M., Moseley, M.E., Kucharczyk, J., 1995. Identification of "premyelination" by diffusion-weighted MRI. J. Comput. Assist. Tomogr. 19, 28–33.
Wolf, N.I., Harting, I., Boltshauser, E., et al., 2005. Leukoencephalopathy with ataxia, hypodontia, and hypomyelination. Neurology 64 (8), 1461–1464.
Wolf, N.I., Harting, I., Innes, A.M., et al., 2007. Ataxia, delayed dentition and hypomyelination: a novel leukoencephalopathy. Neuropediatrics 38 (2), 64–70.
Wolf, N.I., Salomons, G.S., Rodenburg, R.J., et al., 2014. Mutations in RARS cause hypomyelination. Ann. Neurol. 76 (1), 134–139.
Wolfe, C.L., Warrington, J.A., Treadwell, L., Norcum, M.T., 2005. A three-dimensional working model of the multienzyme complex of aminoacyl-tRNA synthetases based on electron microscopic placements of tRNA and proteins. J. Biol. Chem. 280 (46), 38870–38878 (November 18, 2005).
Wolff, S.D., Balaban, R.S., 1989. Magnetization transfer contrast (MTC) and tissue water proton relaxation in vivo. Magn. Reson. Med. 11, 135–144.
Yakovlev, P.I., Lecours, A.R., 1967. The myelogenetic cycles of regional maturation of the brain. In: Minkowski, A. (Ed.), Regional Development of the Brain in Early Life. Blackwell, Oxford, pp. 3–70.
Zara, F., Biancheri, R., Bruno, C., et al., 2006. Deficiency of hyccin, a newly identified membrane protein, causes hypomyelination and congenital cataract. Nat. Genet. 38 (10), 1111–1113.